

Osmund Holm-Hansen · Christopher D. Hewes

## Deep chlorophyll-*a* maxima (DCMs) in Antarctic waters

### I. Relationships between DCMs and the physical, chemical, and optical conditions in the upper water column

Received: 8 January 2004 / Revised: 13 April 2004 / Accepted: 17 May 2004 / Published online: 30 June 2004  
© Springer-Verlag 2004

**Abstract** The US Antarctic Marine Living Resources (AMLR) program has, since 1990, conducted annual surveys from early January through mid-March in a large sampling grid around Elephant Island, Antarctica. Approximately 100 hydrographic stations were occupied twice during each field season, with physical, chemical, optical, and biological data acquired from the surface to 750 m depth or to within 10 m of the bottom at shallower stations. During these 14 years, most of the stations in pelagic waters to the northwest of Elephant Island had very low chlorophyll-*a* (Chl-*a*) concentrations ( $< 0.2 \text{ mg m}^{-3}$ ) in the upper mixed layer (UML) of  $\sim 45 \text{ m}$ , but a deep chlorophyll-*a* maximum (DCM) existed between 50 and 100 m, with a peak at approximately 75 m. This was in contrast to adjacent stations which had higher Chl-*a* concentrations (approximately  $1.0 \text{ mg m}^{-3}$ ) in the UML and no DCM. We provide evidence that the higher Chl-*a* concentrations that occur at depths of 50–100 m result from increased photosynthetic activity and not from a passive sinking of cells from the UML or by the intrusion of Chl-*a* rich coastal waters. Data to support this conclusion include (1) elevated dissolved oxygen concentrations between 50 and 100 m, (2) evidence of active photosynthesis at the depth of the DCM as indicated by increased natural upwelling radiation at 683 nm, and (3) water samples obtained from the DCM at 75 m and incubated under simulated conditions of temperature and light had assimilation numbers of approximately 1.0–1.5 mg carbon fixed per milligram Chl-*a* per hour. DCMs occur in the same

depth range as the temperature minimum layer (TML) (the winter remnant of Antarctic surface water, AASW), which is known to have elevated concentrations of inorganic nutrients essential for growth of phytoplankton. Our data indicate that a DCM develops as a result of (1) depletion of iron (Fe) in the UML with the onset of the summer season, and (2) growth of phytoplankton in the TML where both Fe concentrations and solar irradiance levels are high enough to permit an increase of phytoplankton biomass.

### Introduction

The presence of a deep chlorophyll-*a* maximum (DCM) occurring at depths  $> 50 \text{ m}$  is well known in tropical (Kiefer et al. 1976) and temperate waters (Estrada et al. 1993) and to a lesser extent in Arctic waters (Owrid et al. 2000). In all these studies the occurrence of DCMs is related to depletion of one or more of the major inorganic nutrients (nitrogen, N; phosphorus, P; silicic acid, Si) in the overlying water column. The depth at which DCMs occur in these waters coincides with the nutricline, where the concentration of the limiting nutrient element increases with depth (Cullen and Eppley 1981; Kiefer et al. 1976). Until the report by Holm-Hansen et al. (1994) documenting the occurrence of DCMs in pelagic waters in the Antarctic, most reports of subsurface Chl-*a* in the upper water column in the Southern Ocean showed the maxima to be at depths  $< 40 \text{ m}$  and were ascribed either to effects of photoinhibition, to rare depletion of inorganic N (Holm-Hansen et al. 1989), or possibly as a result of zooplankton grazing pressure in surface waters. Although there are some reports in the literature showing a few station profiles with a DCM in the Southern Ocean, the possible cause or significance of such a deep distribution of Chl-*a* was not discussed (e.g., El-Sayed 1988; Yamaguchi and Shibata 1982). The occurrence of DCMs was previously reported as related

O. Holm-Hansen (✉) · C. D. Hewes  
Marine Biology Research Division,  
Scripps Institution of Oceanography,  
University of California-San Diego,  
La Jolla, CA 92093-0202, USA  
E-mail: oholmhansen@ucsd.edu  
Tel.: +1-858-5342339  
Fax: +1-858-5347313

to the different water types found in the waters around Elephant Island (Holm-Hansen et al. 1994) and could not be explained by limiting concentrations of N, P, or Si, which were  $>25$ , 1.8, and  $40 \mu\text{M}$ , respectively (Silva et al. 1995). Here we describe the geographical distribution of stations where a DCM occurred consistently over a 14-year period during the annual surveys (1990–2003) of the US Antarctic Marine Living Resources (AMLR) program. The depth distribution of Chl-*a* at these stations was analyzed with regard to the physical, chemical, and optical conditions of the water column, and the results provide strong evidence that the DCMs are formed in situ and do not result from intrusion of Chl-*a*-rich coastal waters or passively by cells settling out from the upper mixed layer (UML).

## Materials and methods

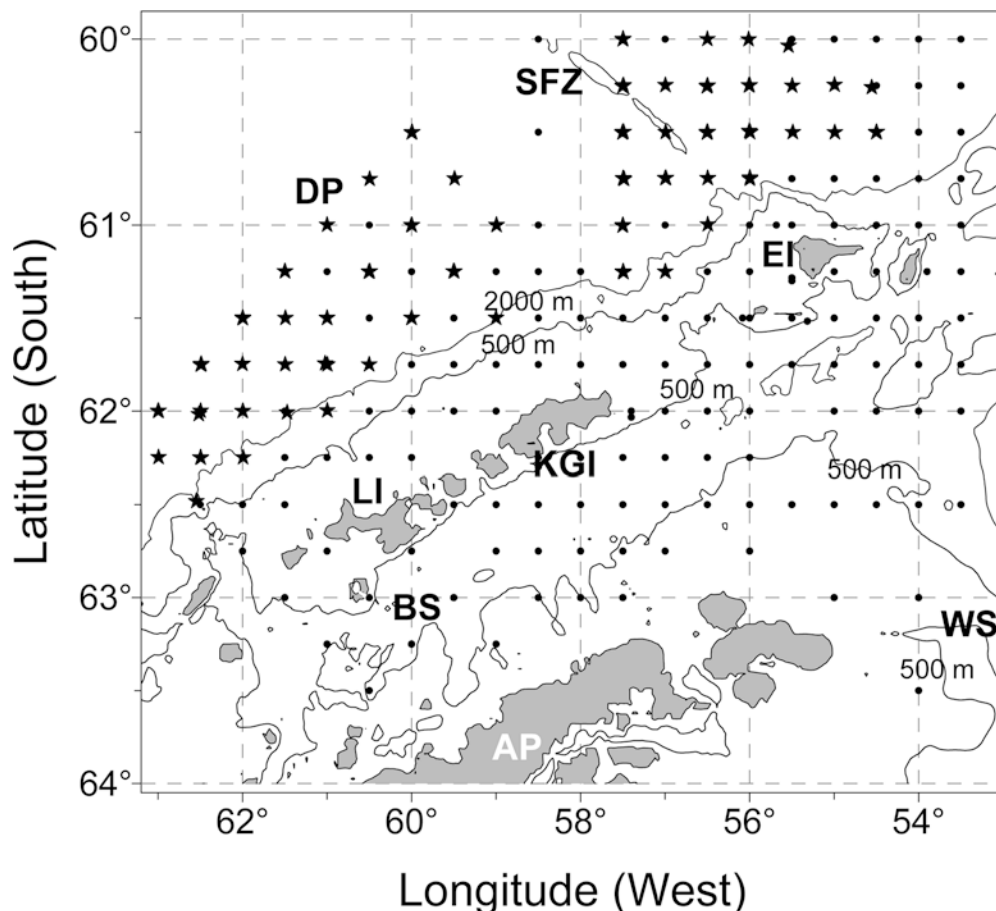
Since the 1989–1990 field season and continuing through the 2002–2003 field season, the AMLR program has conducted two annual survey cruises (with the exception of 1997 and 2000, when only one cruise could be accomplished) in the region north of the Antarctic Peninsula. The two cruises have generally been in the time periods of early January to early February, and mid-February to mid-March of each year, with the same sampling stations occupied for

both of the cruises. The grid of sampling stations which have been occupied during this 14-year time span is shown in Fig. 1. The number of stations occupied during each cruise is close to 100, so not all stations shown in Fig. 1 are occupied during each cruise. During the time period 1990–1995, most stations were in the area surrounding Elephant Island. Since then, fewer stations have been occupied in the Elephant Island area and additional ones added to the north and south of the South Shetland Islands as shown in Fig. 1. All of the above cruises have been done on two research vessels: R.V. “Surveyor” (USA) from 1990 to 1995, and R.V. “Yuzhmorgeologiya” (Russia) from 1996 to 2003.

At each station, an instrumented CTD rosette was deployed to 750 m, or to within 10 m of the bottom at the shallower stations. When the CTD rosette was deployed it was quickly lowered and held at 5-m depth for 3–4 min to allow sensors to equilibrate. In addition to eleven 10-l Niskin bottles equipped with Teflon-covered springs, the following sensors were mounted on the rosette frame:

1. Sea-Bird CTD model SBE-9 PLUS for recording of conductivity, temperature, and depth
2. Sea-Tech transmissometer (25 cm pathlength) for recording of beam attenuation ( $C_t$ ) at 660 nm (only after 1993)

**Fig. 1** Map showing locations of sampling stations occupied by the Antarctic marine living resources (AMLR) program during the years 1990–2003. Stars indicate stations which were used for the data shown in Fig. 2; filled circles show location of stations where no deep chlorophyll-*a* maximum (DCM) have been recorded. The continuous lines show the 500- and 2,000-m isopleths. DP Drake Passage, SFZ Shackleton Fracture Zone, EI Elephant Island, KGI King George Island, LI Livingston Island, BS Bransfield Strait, AP Antarctic Peninsula, WS Weddell Sea



3. Sea-Tech pulsed fluorometer for estimation of Chl-*a* concentrations (only after 1992)
4. Biospherical Instruments solar irradiance sensor (model QCP-200 L) with a cosine response for recording of attenuation of photosynthetically available radiation (PAR) with depth (only after 1993)
5. Seabird oxygen electrode (SBE 13-02-B prior to 2003, SBE 43 after Leg II, 2003) Data from all sensors were acquired on both the downcast and upcast by a computer connected to the Sea-Bird deck unit; however, only data from downcasts was used for examining physical, optical and oxygen concentration characteristics of the water column. Niskin bottles were triggered at discrete depths during the upcast to obtain water samples for Chl-*a* determination, as well as for salinity and oxygen for checking sensor calibration (see Amos 2001). Water samples obtained on the upcasts were at standard target depths of 750, 200, 100, 75, 50, 40, 30, 20, 15, 10, and 5 m. Incident solar radiation (PAR) was also monitored and recorded continuously with a 2-pi sensor (BSI, model QSR-240, from 1992 to 1999; Licor sensor, from 2000 to 2003) mounted in a shade-free location on the ship's superstructure.

For determination of Chl-*a* concentrations in the water samples, 100 ml aliquots were filtered at a pressure differential of <150 mm Hg through a 25-mm glass fiber filter (Whatman GF/F), which was then placed in 10 ml of absolute methanol (Holm-Hansen and Riemann 1978). After extraction in the dark for at least 2 h, Chl-*a* concentrations were determined by measurements of Chl-*a* fluorescence (Holm-Hansen et al. 1965) in a Turner Designs fluorometer (model no. 700), which had been calibrated against purified Chl-*a* (Sigma C-6144) and the instrument response checked daily with a coproporphyrin standard (Sigma C-4529) and/or with a solid state fluorescence standard (Turner Designs no. 7000-994).

During the AMLR 1994 field season a profiling radiometer (BSI, model PUV-500) was lowered by hand for measurement of downwelling irradiance (PAR) and upwelling radiance at 683 nm as a function of depth. Data were recorded at the rate of once per second by computer. As downwelling solar irradiance at 683 nm can be detected to approximately 5 m, only data from >7 m depth were considered. A profile of photosynthesis in the water column was limited to ~90 m due to the length of the cable. Measurement and interpretation of instantaneous in situ rates of photosynthesis have been described by Gordon (1979), Kiefer et al. (1989), Chamberlin et al. (1990), Chamberlin and Marra (1992), and Marra et al. (1992, 1993).

Water samples for determination of the rate of photosynthesis relative to irradiance (P vs I) were obtained from depths of 5–75 m at stations having a DCM and also from contiguous stations not showing any DCM. Eighteen 50-ml polycarbonate tubes (with leakproof screw caps) were filled with water from each sampled

depth and inoculated with 5  $\mu\text{Ci}$   $\text{NaH}^{14}\text{CO}_3$  (0.185 mBq). Two of the tubes were wrapped with black tape and aluminum foil for measurement of dark fixation of radiocarbon. Two tubes were exposed to full sunlight, and the remaining 14 tubes were covered with neutral density filters so that the samples were exposed to approximately 50, 25, 12, 6, 3, 1.5, and 0.75% of incident solar radiation. All sample tubes were incubated in a water bath in a shade-free location on the deck of the ship. The water temperature was maintained close to surface temperature values with running surface sea water. Each incubation lasted 6–10 h, centered around local noon. The integrated PAR during the incubation period was obtained from the integrating PAR sensor, which was mounted in close proximity to the incubation unit. After incubation the samples were filtered through glass fiber filters (Whatman GF/F, 25 mm), which were placed in scintillation vials and exposed to HCl fumes for 6–8 h. The filters were then dried and the fixed radiocarbon measured by standard liquid scintillation techniques.

Only 3 years (1997–1999) are represented in Fig. 2, as these provided complete sets of the multiple types of data that we discuss. Other years did not include data from one or more of the profiling sensors (fluorometer, transmissometer, oxygen electrode, or PAR meter) and P vs I was discontinued after 1999. Our conclusions regarding the consistency of the DCM at stations in the northwestern region of the sampling grid are well documented for all 14 years, however, by our data on extracted Chl-*a* concentrations in the upper 200 m of the water column and the various in situ profiling sensors used.

## Results

### Water column characteristics

Data in Fig. 2 show water column characteristics at 62 stations where DCMs occurred between 50 and 100 m as contrasted to water column characteristics at 20 stations, which were in close proximity to the stations with a DCM, but had maximal Chl-*a* concentrations in the UML and no DCM. Stations with a DCM have low Chl-*a* concentrations in the UML and maximal concentrations at depths close to 75 m (Fig. 2a). The Chl-*a* concentrations in these DCMs, however, are lower than the Chl-*a* concentrations in the UML at adjacent stations which had no DCM (Fig. 2b). The contrasting distributions of Chl-*a* concentrations in the upper water column for these two groups of stations are consistent with the Chl-*a* profiles as determined with the in situ fluorometer (Fig. 2c, d) and with beam attenuation coefficients ( $C_t$ ) determined with the transmissometer (Fig. 2e, f).

The phytoplankton comprising the DCM were metabolically active as indicated by the distribution of oxygen, and are not merely senescent cells sinking in

**Fig. 2a–r** Water column characteristics at 62 stations with DCMs (figures to the *left*) and at 20 contiguous stations without any DCMs (figures to the *right*) from the 1997 to 1999 field seasons. Data for individual stations are indicated with *small circles* or with *light lines*; the mean value is shown by the *dark line*. **a** and **b** Chlorophyll-*a* (Chl-*a*) concentrations, **c** and **d** in situ fluorescence recorded with the profiling fluorometer, **e** and **f** beam attenuation ( $C_t$ ) recorded with the profiling transmissometer, **g** and **h** oxygen concentrations recorded with a profiling oxygen sensor, **i** and **j** attenuation of photosynthetically available radiation (PAR) in the water column. The *dashed vertical lines* indicate the percent of surface irradiance at depths of 47, 75, and 120 m, **k** and **l** temperature, **m** and **n** salinity, **o** and **p** water density ( $\sigma_t$ ), **q** and **r** temperature-salinity diagrams

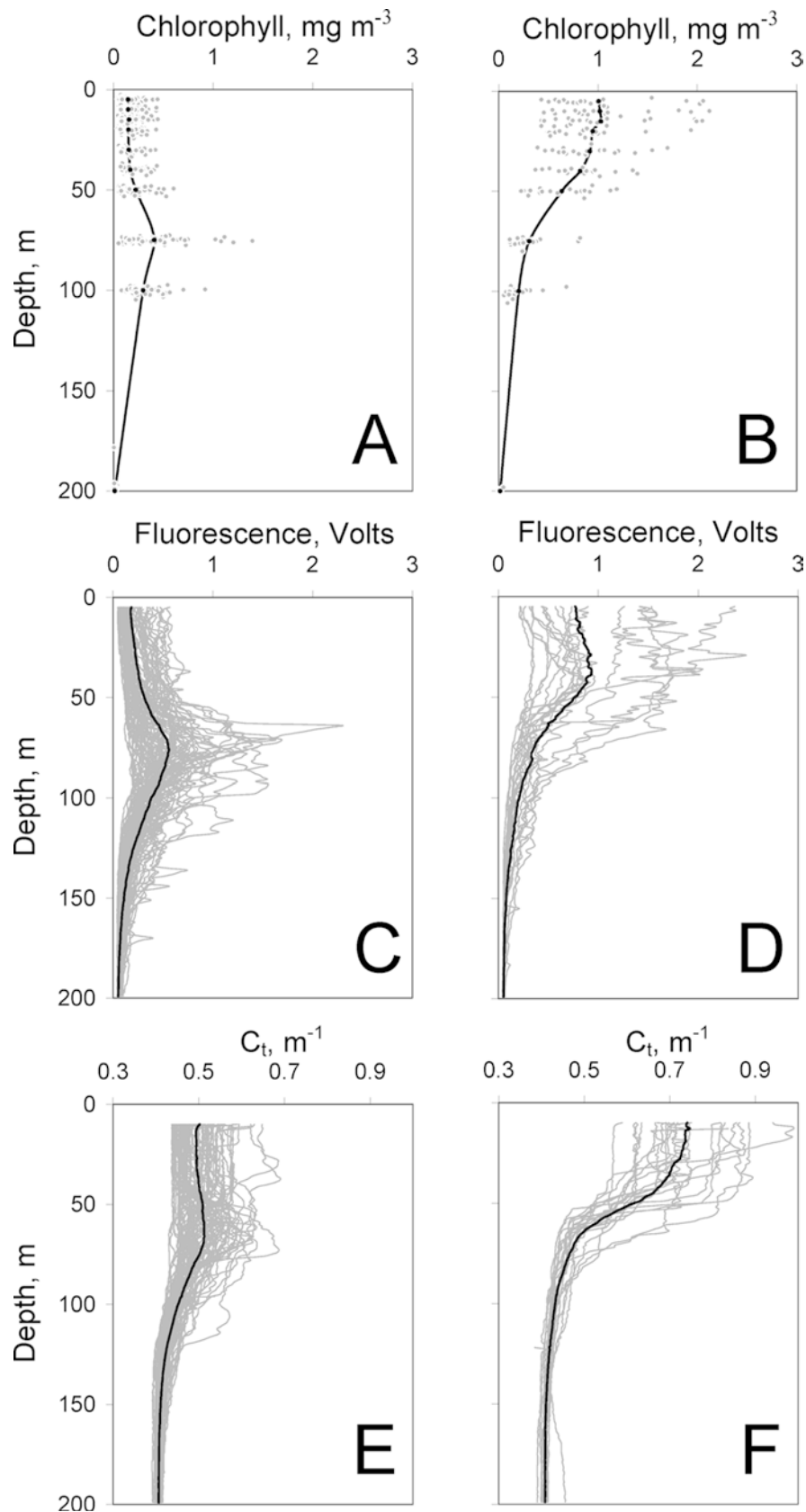
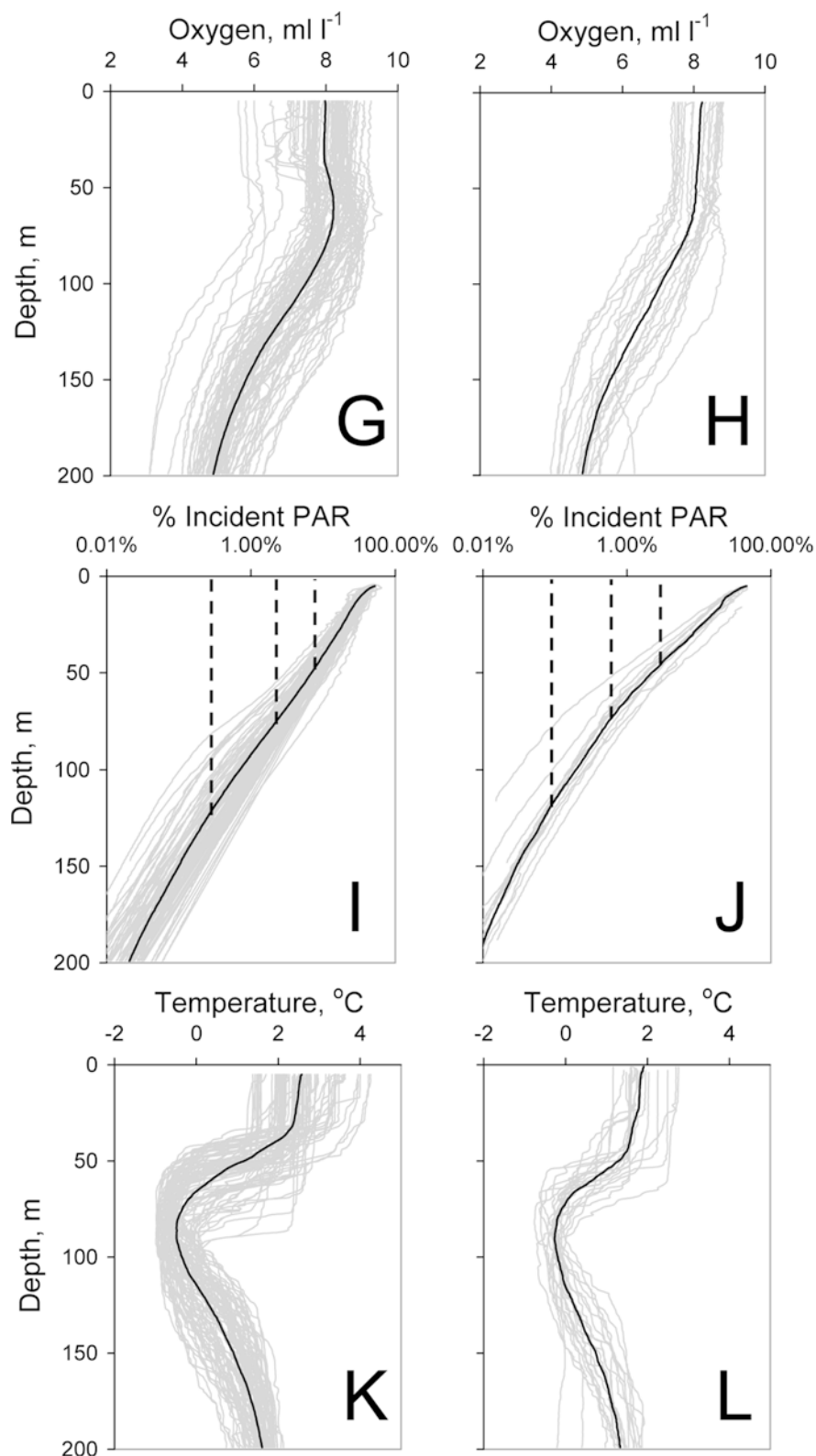


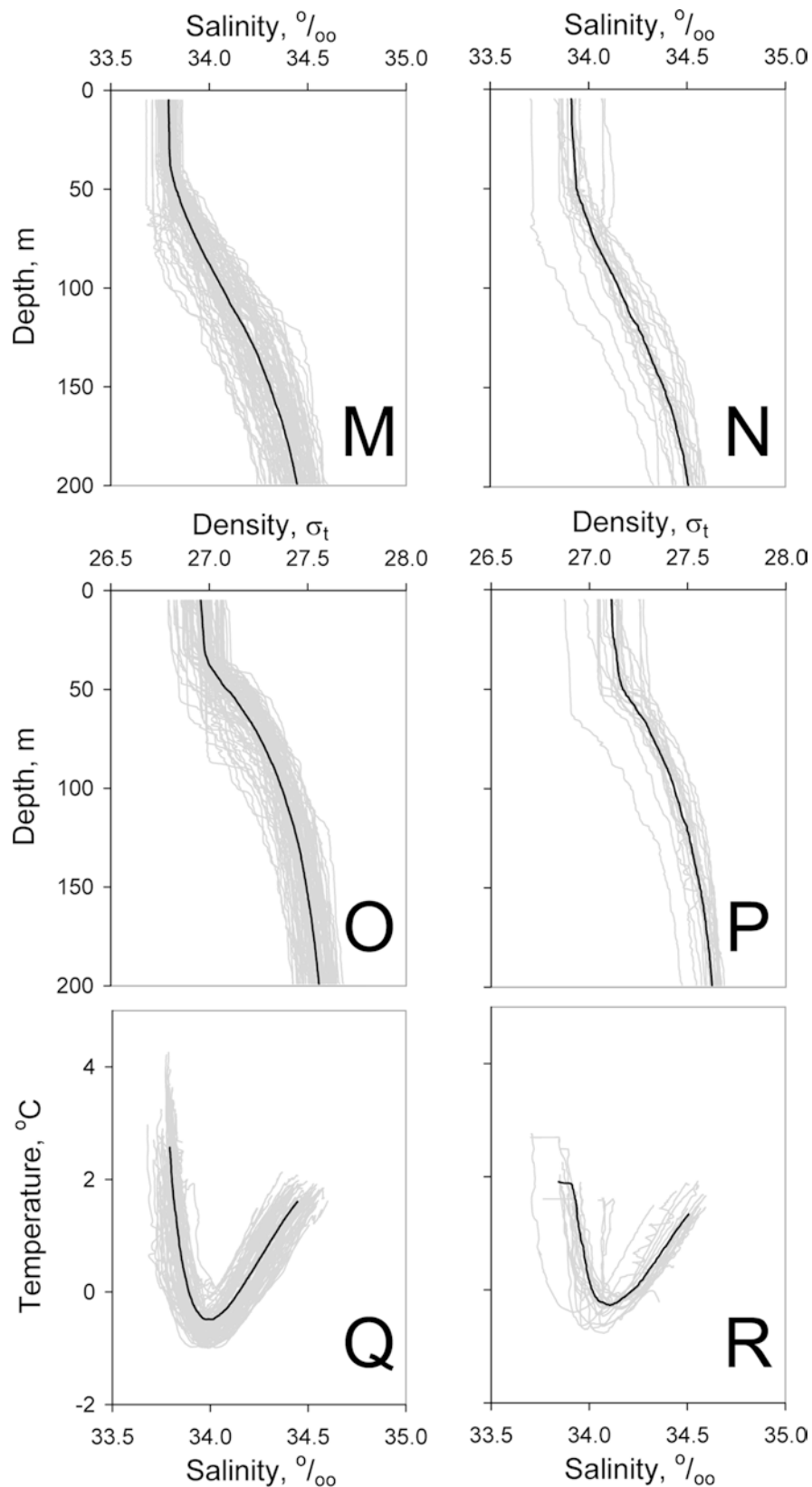
Fig. 2g–L  
(Contd.)



the water column and concentrating in the winter water. There is a peak in oxygen concentration at approximately 75 m depth (Fig. 2g) for the stations having a DCM, in contrast to those stations where a DCM was not found (Fig. 2h). The elevated oxygen

concentrations between 50 and 100 m at the stations with a DCM (Fig. 2g; compare with oxygen profile in Fig. 2h) are most likely the result of photosynthesis occurring within that depth range with the following considerations:

**Fig. 2m-r**  
(Contd.)



1. The attenuation curves for PAR in the upper water column are shown as percent of incident radiation (Fig. 2i, j). The value for mean daily radiation (measured as Einsteins, E) incident upon the sea

surface ( $I_0$ ) during January and February is  $37 \text{ E m}^{-2}$  as recorded by our deck PAR sensor. Assuming an average of 15 h of daylight per day, the mean daily irradiance at the sea surface is approximately

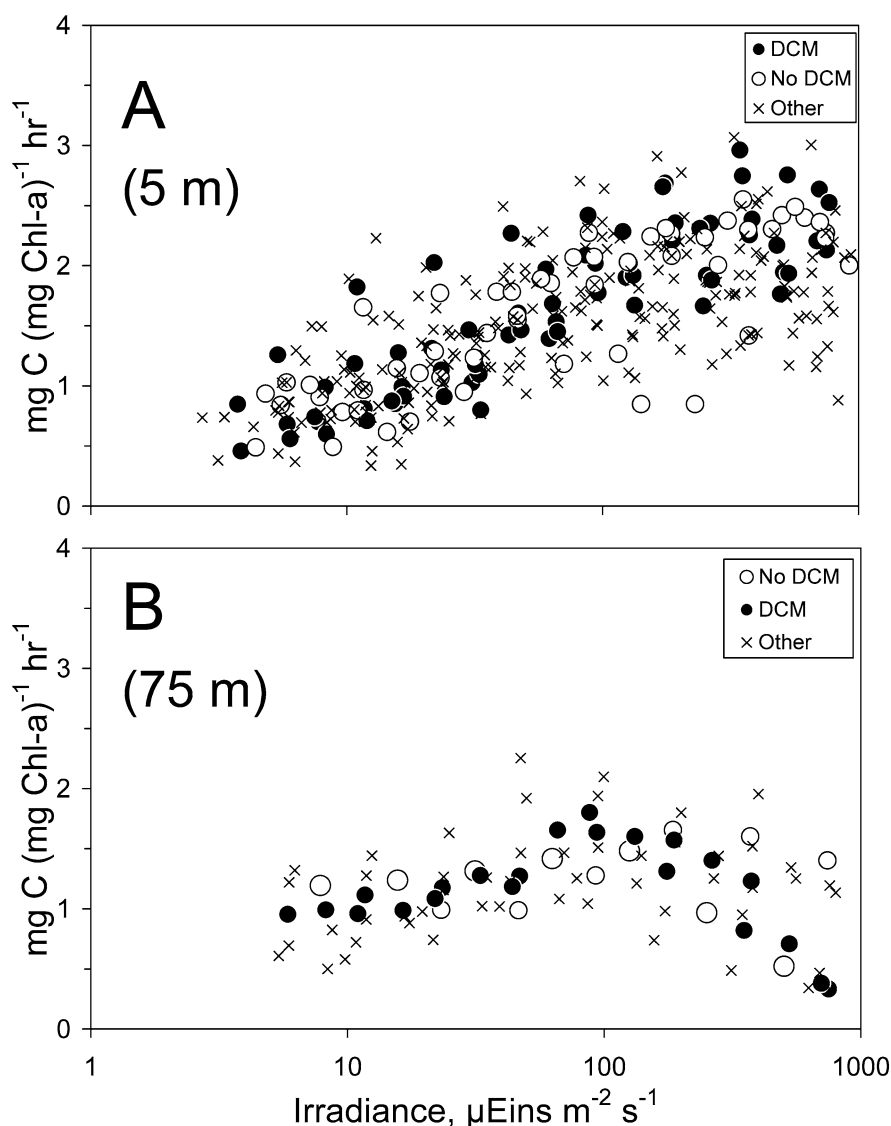
$680 \mu\text{E m}^{-2} \text{s}^{-1}$ . It is seen that the attenuation curve (Fig. 2i) shows inflection points at approximately 47 m (where Chl-*a* concentrations start to increase) and at 120 m (close to the bottom of the DCM). The irradiance values at the top (47 m), middle (75 m), and bottom (120 m) of the DCM are approximately 7.8, 2.3, and  $0.3\%$  of  $I_0$ , respectively, which equates to approximately 53, 15, and  $2.0 \mu\text{E m}^{-2} \text{s}^{-1}$ . The corresponding irradiance values at 47, 75, and 125 m for the stations without a DCM are 18, 4.0, and  $0.7 \mu\text{E m}^{-2} \text{s}^{-1}$ , respectively.

- Measurements of photosynthesis as a function of the irradiance ( $P$  vs  $I$ ) indicate no significant difference in the assimilation numbers (AN; milligram C fixed per milligram Chl-*a* per hour) for either the 5 or 75 m water samples of stations with or without a DCM (Fig. 3). These data demonstrate that the only difference in rates of photosynthesis between populations with or without a DCM will be a function of the in situ light intensity. The light saturation value ( $I_k$ ) is

approximately  $100 \mu\text{E m}^{-2} \text{s}^{-1}$  for both the 5- and 75-m depths. Photosynthetic rates at irradiances below this  $I_k$  value will be light-limited. The maximal photosynthetic rates, however, are higher for the 5-m samples (AN of approximately 2.0) as compared to the AN of approximately 1.5 for the 75-m samples. The photoinhibition response of the phytoplankton at 75 m is pronounced, with a rapid decrease in the AN at irradiances higher than about  $100 \mu\text{E m}^{-2} \text{s}^{-1}$ . Photoinhibition is much less pronounced in the samples from 5 m, as inhibition is evident only at irradiances close to  $1,000 \mu\text{E m}^{-2} \text{s}^{-1}$ .

- Data of increased upwelling radiance (683 nm) correspond with elevated oxygen concentrations between depths of 50 and 100 m (Fig. 4). The profiles for Chl-*a* concentrations and solar radiation (Fig. 4a) resemble the stations with a DCM shown in Fig. 2. The 683 nm upwelling data (Fig. 4b) give evidence that the rate of in situ photosynthesis (see Materials and methods for references) decreases with depth in

**Fig. 3a, b** Photosynthesis versus irradiance data for phytoplankton in the AMLR study area. **a** Samples obtained from 5 m depth. **b** Samples obtained from 75 m depth. Filled circles represent stations with a DCM, empty circles represent stations having a temperature minimum but without a DCM, xs are all other stations in the AMLR survey area



the UML (0–45 m) and then increases to a secondary maximum at approximately 70 m. Below 70 m, the upwelling radiance of 683 nm decreases rapidly, in contrast to the profile of Chl-*a* concentrations. The depth interval where the 683 nm upwelling radiation indicates enhanced photosynthetic rates is within the low temperature minimum layer (TML) and also coincides with the depths having increased oxygen concentrations (Fig. 4b).

#### Location of stations with a DCM

Profiles of temperature (Fig. 2k, l), salinity (Fig. 2m, n), density (Fig. 2o, p), as well as the temperature/salinity diagrams (Fig. 2q and r) all indicate that the physical characteristics of the water column at the contiguous stations differ slightly as compared to the data from the stations having a DCM. Presumably this is the result of some mixing of Drake Passage waters (which have a DCM) with waters originating from Bransfield Strait or the Weddell Sea, which are slightly colder and more saline than Drake Passage waters. Locations of stations where DCMs are routinely found are in the northwestern area of the AMLR sampling grid as shown in Fig. 5. Not all stations within the demarcation line in Fig. 5 have a DCM in all years. For instance, the three stations within area A and the eight stations within area B of Fig. 5 occasionally do not have a DCM. The anomalous distributions of Chl-*a* at the stations within area A in

1998 and 2000 were surprising, as the contiguous stations to the east, south, and west all had a pronounced DCM. The physical and biological characteristics of the upper water column at those stations within area A indicated considerable mixing as the TML was markedly eroded, the T/S diagrams were consistent with type 2 or type 3 waters as described by Amos (2001), and the silicic acid concentrations were significantly higher (approximately 44  $\mu\text{M}$ ) as compared to approximately 35  $\mu\text{M}$  at adjacent stations with a DCM. The Chl-*a* concentrations at 5 m depth at the stations within area A during 1998 and 2000 were  $\sim 1.0 \text{ mg m}^{-3}$ , as compared to Chl-*a* values of  $\sim 0.1 \text{ mg m}^{-3}$  at stations that had a DCM. These changes in the upper water column could be the result of either horizontal mixing with coastal waters or from vertical mixing with deeper water but the former seems more likely, however, as the T/S diagrams at these stations without a DCM indicated a mixture of Drake Passage waters with waters from the Bransfield Strait or the Weddell Sea as described by Amos (2001).

#### Discussion

The oceanographic characteristics of the AMLR sampling area are complex due to the mixing of different water masses, the presence of extensive continental shelves, and deep currents of pelagic waters impacting bathymetric features such as the Shackleton Fracture

**Fig. 4a, b** Water column characteristics at station D004 (February 1994) showing enhanced photosynthetic rates in the DCM depth range. **a** Profiles of extracted Chl-*a* concentrations (filled circles), in situ fluorescence (FI), and attenuation of solar radiation (PAR). The vertical lines with arrows show the depths and corresponding solar irradiance at those depths for the top, mid-point, and bottom of the DCM. **b** Profiles of relative rates of photosynthesis as measured by upwelling radiance at 683 nm (P), oxygen concentration ( $\text{O}_2$ ), and temperature (T)

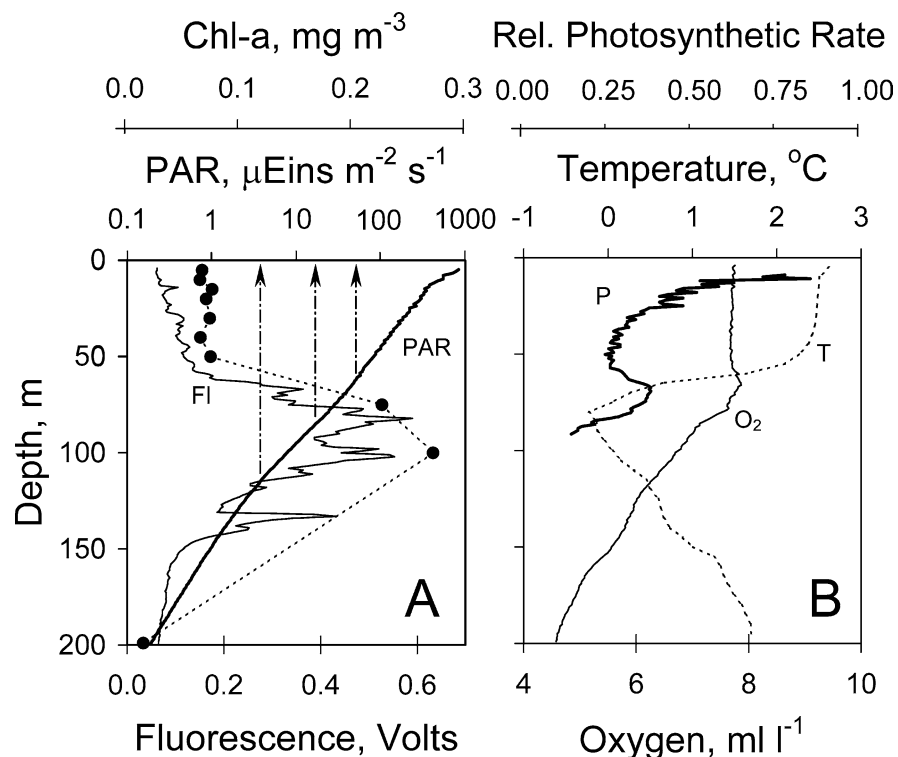
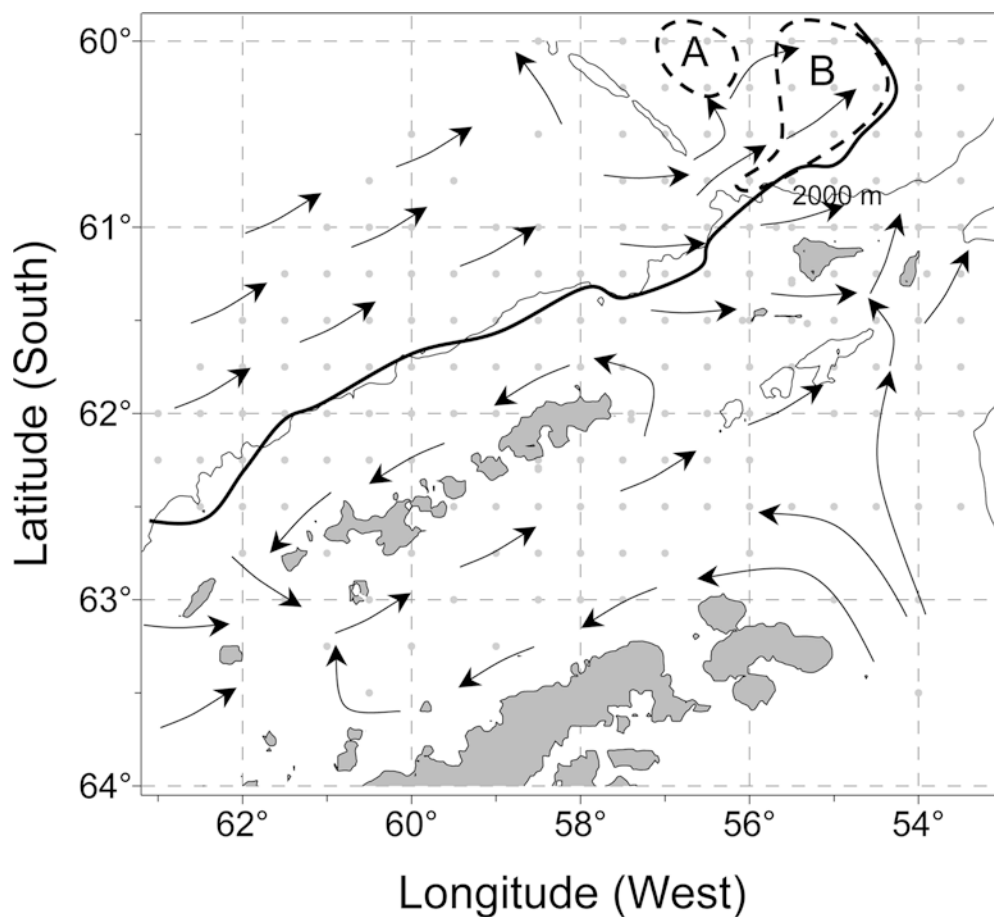


**Fig. 5** Map of the AMLR sampling grid, showing the region where DCMs are usually found (entire northwest region of sampling grid as demarcated by the *dark continuous line*). Stations within areas A and B (enclosed within *dashed lines*) occasionally show mixing with coastal waters and do not have a DCM. The *thin continuous line* is the 2,000 m isopleth. Arrows indicate direction of surface water flow as described by Hofmann et al. (1996), Stein (1988), Siegel (1988), and Zhou et al. (2002), in addition to drifter buoy tracks (AMLR, unpublished data)



Zone (Stein 1988; Amos 2001). Of all the stations in the AMLR grid, the only stations that consistently have a DCM are located in the northwest region of the AMLR sampling grid as shown in Fig. 5. T/S diagrams indicate that these DCM stations are typical of Drake Passage waters, while all other stations lacking a DCM have T/S diagrams characteristic of water from either Weddell Sea or Bransfield Strait, or mixtures with Drake Passage waters (Holm-Hansen et al. 1997; Amos 2001). The presence of a DCM is generally ascribed to either active phytoplankton growth at depth in situ, or as a result of downward advection of Chl-*a* rich waters from coastal regions. Analysis of the physical oceanographic data from the 14 years of the AMLR program, however, does not provide any evidence that would support the hypothesis that the DCM is due to lateral intrusion of waters from coastal regions with high Chl-*a* concentrations.

#### Data in support of in situ formation of the DCM

The data shown in Fig. 2 provide convincing evidence that the DCM found between 50 and 100 m depth is the result of phytoplankton growth and photosynthesis in situ within that depth range. The evidence that these DCMs are a function of elevated in situ photosynthetic activity includes:

1. Dissolved oxygen concentrations at the stations with a DCM had uniform concentrations in the UML (approximately 45 m), but higher concentrations between 50 and 100 m, corresponding to the depth range of the DCM (Fig. 2g). Such an increase in oxygen relative to concentrations in the UML was not present at adjacent stations lacking a DCM (Fig. 2h). The increased oxygen concentrations within a DCM are most likely the result of active photosynthesis within that depth range. If it were not, oxygen concentration would be expected to have a uniform distribution within the winter water or be maximal at the temperature minimum since its saturation is inversely proportional to water temperature.
2. Phytoplankton sampled from the DCM have the capacity for high rates of photosynthesis as indicated by photosynthetic assimilation numbers of approximately 1.5 at the  $I_k$  value of approximately  $100 \mu\text{E m}^{-2} \text{s}^{-1}$  (Fig. 3). The in situ irradiances at the top, middle, and bottom of the DCM (53, 15, and  $2.0 \mu\text{E m}^{-2} \text{s}^{-1}$ , respectively) are sufficiently high to permit net photosynthesis to occur, even though they are in the light-limiting range for photosynthesis. The irradiance at 120 m is just slightly higher than the value of  $1.0 \mu\text{E m}^{-2} \text{s}^{-1}$ , which is the lowest light level at which net radiocarbon fixation might be detected by in situ incubations of water samples in the Bransfield Strait region (Holm-Hansen and Mitchell

- 1991). Photosynthetic rates of the phytoplankton within the DCM, given the in situ light regime, would thus be close to maximal at the top of the DCM (~47 m) and very low at 120 m. Such a profile of photosynthetic rates is predicted given the profile of elevated oxygen at these depths (Fig. 2g) as well as the profile of upwelling radiation at 683 nm (Fig. 4b). This is not the case for populations with high Chl-*a* concentrations in the UML that significantly attenuate incident irradiance (Fig. 2j) such that relatively low photosynthetic rates would occur in winter water.
3. Measurement of 683 nm upwelling radiation (Fig. 4b) also shows a marked increase in photosynthesis within the DCM. The profile for upwelling radiation at 683 nm (Fig. 4b) does not track the Chl-*a* profile (Fig. 4a), but is similar to the profile of elevated oxygen concentration that is most pronounced in the depth range of 50–80 m (Figs. 4b and 2g).

### Nutrient limitation in waters with a DCM

It is unlikely that concentrations of inorganic N, P, or Si are limiting phytoplankton biomass at the stations with a DCM. Concentrations of N, P, and Si are approximately 26, 1.5, and 30  $\mu\text{M}$ , respectively, in the upper 50 m of the water column, with concentrations increasing below 50 m (Silva et al. 1995; Holm-Hansen et al. 1997). These concentrations are considerably higher than the concentrations required to support the biomasses of phytoplankton measured in the region. This is similar to other areas of high nutrient, low chlorophyll (HNLC) conditions in the world ocean (Chisholm and Morel 1991).

There are convincing data, however, that availability of iron (Fe) limits phytoplankton biomass in many pelagic regions of the Southern Ocean (Hoppema et al. 2003). These data include results from enrichment cultures (e.g., Martin et al. 1990a) as well as documenting increased phytoplankton biomass in situ following addition of large amounts of Fe salts to surface waters (e.g., Boyd et al. 2000). Although there have been many studies reporting dissolved Fe concentrations in Antarctic waters (summarized in de Baar and de Jong 2001), the only data from within or close to the AMLR region are those of Martin et al. (1990b), who reported low Fe concentrations (0.1–0.16 nM) in pelagic surface waters (which had a temperature minimum) immediately west of the AMLR sampling grid and high concentrations of Fe (4–8 nM) in Gerlache Strait. Sañudo-Wilhelmy et al. (2002) have also reported high Fe concentrations at Palmer Station (4–6 nM) and at Deception Island within Bransfield Strait (31 nM). Waters from the central and western Weddell Sea, which flow into the eastern portions of the AMLR sampling grid, also have relatively high Fe concentrations of  $>1.0$  nM (Sañudo-Wilhelmy et al. 2002; Westerlund and Öhman 1991). All these data on Fe concentrations are consistent with the conclusion

that Fe limits phytoplankton biomass in pelagic Antarctic waters which have low Chl-*a* concentrations in surface waters (approximately  $<0.4$  mg  $\text{m}^{-3}$ ), but generally is not a limiting nutrient for phytoplankton in coastal waters. The only enrichment studies that have been made in the AMLR study area are those of Helbling et al. (1991), which demonstrated that the addition of Fe to surface waters from stations having a DCM resulted in increased phytoplankton biomass, but no differences were found for stations without a DCM.

These historical studies strongly suggest that Fe is limiting phytoplankton biomass in the UML of HNLC regions of the AMLR survey area. The question then arises as to why there is a DCM at these stations, and if phytoplankton at that depth are Fe-stressed to the same extent as the phytoplankton in the UML. Chemostat theory (Veldkamp 1976) dictates that nutrients will limit phytoplankton biomass but not growth rate. This view is substantiated in natural systems by classical studies of macronutrient-limited waters (e.g., Goldman et al. 1979; Goldman 1980) in which growth rates are maximized through regeneration processes at the expense of the total biomass and size-structure of a community. Thus the fact that assimilation numbers were approximately the same for samples from stations with or without a DCM (see Fig. 3) does not argue against nutrient limitation of the phytoplankton at the stations with a DCM. The fact that Chl-*a* concentrations within the DCM are much higher than in the UML suggests that the limiting nutrient (presumably Fe) is in higher concentrations at depths between 50 and 100 m, which corresponds to the location of the TML. Those stations without a DCM would probably have similar limiting nutrient concentrations in the TML; however there is simply not enough light reaching these depths to promote significant rates of photosynthesis for growth (e.g., Sverdrup 1953).

### Significance of the temperature minimum layer

The data in Figs. 2a, k and 4 show that the DCM is found in the same depth interval as the TML. This TML is the remnant of Antarctic Surface Water (AASW) from the winter period when the UML is deeply mixed ( $>150$  m) and uniform in regard to temperature and nutrients. During the formation of this deeply mixed water column during the winter months, solar radiation is very low, which will result in low phytoplankton biomass and relatively little assimilation of inorganic nutrients. At the same time, Fe concentrations will increase throughout the UML by aeolian deposition, continued input from coastal waters, and by mixing with deeper waters which have higher Fe concentrations (Measures and Vink 2001). The dissolved oxygen content and inorganic nutrient concentrations are thus high in this winter water (Sievers and Nowlin 1988; Hoppema et al. 2003). In late winter and early spring, the UML will get shallower as described by Kiefer and Kremer (1981) for temperate waters, followed by formation of a relatively shallow UML due to solar

heating (Deacon 1937). With increasing solar radiation in spring, Fe concentrations in this UML should decrease due to assimilation by phytoplankton and subsequent loss of phytoplankton biomass by macro-zooplankton grazing. The result would be low Fe concentrations in the UML, with higher Fe concentrations remaining in the TML between 50 and 100 m.

During summertime the rate of primary production in the euphotic zone would still be maximal in the UML (which is ~45 m in the AMLR study area) due to microbial processes which would effectively recycle essential inorganic nutrients. Pelagic Antarctic waters have an active microbial food web (Hewes et al. 1985) as also evidenced by very high concentrations of ammonia (Rönnner et al. 1983). The low Fe concentrations in the UML, however, would result in low phytoplankton biomass as evidenced in other HNLC regions (Chisholm and Morel 1991). Our data on attenuation of solar radiation in the water column show that the growth rate of the phytoplankton residing within the TML will be severely light limited, in contrast to conditions in the UML where light levels are high. The higher Fe concentrations in the remnant of winter water would, however, result in increased phytoplankton biomass where irradiances may be low, but still higher than the compensating light irradiance value, that would occur at depths between 100 and 125 m.

**Acknowledgements** This work was funded through the US AMLR program, administered by the Antarctic Ecosystem Research Division at NOAA's Southwest Fisheries Research Center, La Jolla, California. Special funds were also provided by NOAA/AMLR to compile a rational data base of all our data to present, and without which this manuscript could not have been accomplished. Reiner Schlitzer produced Ocean Data View, which was a most invaluable tool in our analyses of water column profile data. We thank all officers and crews of the R.V. "Surveyor" and R.V. "Yuzhmorgeologiya", for their excellent help during all field operations, and also all other AMLR personnel who assisted us on board ship. Special thanks are extended to Tony Amos, who acquired and processed the physical oceanographic data. We also thank Mati Kahru and B. Greg Mitchell for providing us with solar irradiance data acquired with their free fall optical profiling instrumentation. We also thank three anonymous reviewers for their helpful comments.

## References

- Amos AF (2001) A decade of oceanographic variability in summertime near Elephant Island, Antarctica. *J Geophys Res* 106:22401–22423
- Baar HJW de, de Jong JTM (2001) Distributions, sources and sinks of iron in seawater. In: Turner DR, Hunter KA (eds) *The biogeochemistry of iron in seawater*. Wiley, New York, pp 123–253
- Boyd PW, et al (2000) A mesoscale phytoplankton bloom in the polar Southern Ocean stimulated by Fe fertilization. *Nature* 407:695–702
- Chamberlin WS, Marra J (1992) Estimation of photosynthetic rate from measurements of natural fluorescence: analysis of the effects of light and temperature. *Deep-Sea Res* 39:1695–1706
- Chamberlin WS, Booth CR, Kiefer DA, Morrow JH, Murphy RC (1990) Evidence for a simple relationship between natural fluorescence, photosynthesis and chlorophyll in the sea. *Deep-Sea Res* 37:951–973
- Chisholm SW, Morel FMM (1991) What controls phytoplankton production in nutrient-rich areas of the open sea? *Limnol Oceanogr* 36:1507–1970
- Cullen JJ, Eppley RW (1981) Chlorophyll maximum layers of the Southern California Bight and possible mechanisms of their formation and maintenance. *Oceanol Acta* 4:23–32
- Deacon GER (1937) The hydrology of the Southern Ocean. *Discov Rep* 15:1–124
- El-Sayed SZ (1988) Seasonal and interannual variabilities in antarctic phytoplankton with reference to krill distribution. In: Sahrhage D (ed) *Antarctic Ocean and resources variability*. Springer, Berlin Heidelberg New York, pp 101–119
- Estrada MC, Marras M, Latasa E, Berdalet M, Delgado M, Riera T (1993) Variability of deep chlorophyll maximum characteristics in the Northwestern Mediterranean. *Mar Ecol Prog Ser* 92:289–300
- Goldman JC (1980) Physiological processes, nutrient availability, and the concept of relative growth rate in marine phytoplankton ecology. In: Falkowski P (ed) *Primary productivity in the sea*. Plenum, New York, pp 179–194
- Goldman JC, McCarthy JJ, Peavey DC (1979) Growth rate influence on the chemical composition of phytoplankton in oceanic waters. *Nature* 279:210–215
- Gordon HR (1979) Diffuse reflectance of the ocean: the theory of its augmentation by chlorophyll-*a* fluorescence at 685 nm. *Appl Opt* 18:1161–1166
- Helbling EW, Villafañe V, Holm-Hansen O (1991) Effect of Fe on productivity and size distribution of Antarctic phytoplankton. *Limnol Oceanogr* 36:1879–1885
- Hewes CD, Holm-Hansen O, Sakshaug E (1985) Alternate carbon pathways at lower trophic levels in the Antarctic foodweb. In: Siegfried WR, Condy PR, Laws RM (eds) *Antarctic nutrient cycles and food webs*. Springer, Berlin Heidelberg New York, pp 277–283
- Hofmann EE, Klinck JM, Lascara CM, Smith DA (1996) Water mass distribution and circulation west of the Antarctic Peninsula and including Bransfield Strait. In: Ross RM, Hofmann EE, Quetin LB (eds) *Foundations for ecological research west of the Antarctic Peninsula*. American Geophysical Union, Washington, pp 61–80
- Holm-Hansen O, Mitchell BG (1991) Spatial and temporal distribution of phytoplankton and primary production in the western Bransfield Strait region. *Deep-Sea Res* 38:961–980
- Holm-Hansen O, Riemann B (1978) Chlorophyll *a* determination: improvements in methodology. *OIKOS* 30:438–447
- Holm-Hansen O, Lorenzen CJ, Holmes RW, Strickland JDH (1965) Fluorometric determination of chlorophyll. *Cons Perm Int Explor Mer* 30:3–15
- Holm-Hansen O, Mitchell BG, Hewes CD, Karl DM (1989) Phytoplankton blooms in the vicinity of Palmer station, Antarctica. *Polar Biol* 10:49–57
- Holm-Hansen O, Amos AF, Silva N, Villafañe V, Helbling EW (1994) In situ evidence for a nutrient limitation of phytoplankton growth in pelagic Antarctic waters. *Antarct Sci* 6:315–324
- Holm-Hansen O, Hewes CD, Villafañe VE, Helbling EW, Silva N, Amos AF (1997) Distribution of phytoplankton and nutrients in relation to different water masses in the area around Elephant Island, Antarctica. *Polar Biol* 18:145–153
- Hoppema M, de Baar HJW, Fahrbach E, Hellmer HH, Klein B (2003) Substantial advective iron loss diminishes phytoplankton production in the Antarctic zones. *Global Biogeochem Cycle* 17:1025.01–1025.09
- Kiefer DA, Kremer JN (1981) Origins of vertical patterns of phytoplankton and nutrients in the temperate, open ocean: a stratigraphic hypothesis. *Deep-Sea Res* 28A:1087–1105
- Kiefer DA, Olson RJ, Holm-Hansen O (1976) Another look at the nitrite and chlorophyll maxima in the central North Pacific. *Deep-Sea Res* 23:1199–1208
- Kiefer DA, Chamberlin WS, Booth CR (1989) Natural fluorescence of chlorophyll *a*: relationship to photosynthesis and chlorophyll concentration in the western South Pacific gyre. *Limnol Oceanogr* 34:868–881

- Marra J, Dickey T, Chamberlin W, Ho C, Granata T, Kiefer D, Langdon C, Smith R, Baker K, Bidigare R, Hamilton M (1992) The estimation of seasonal primary production from moored optical sensors in the Sargasso Sea. *J Geophys Res* 97:7399–7412
- Marra J, Chamberlin WS, Knudson C (1993) Proportionality between in situ carbon assimilation and bio-optical measures of primary production in the Gulf of Maine in summer. *Limnol Oceanogr* 3:231–238
- Martin JH, Fitzwater SE, Gordon RM (1990a) Iron deficiency limits phytoplankton growth in Antarctic waters. *Global Biogeochem Cycle* 4:5–12
- Martin JH, Gordon RM, Fitzwater SE (1990b) Iron in Antarctic waters. *Nature* 345:156–158
- Measures CI, Vink S (2001) Dissolved Fe in the upper waters of the Pacific sector of the Southern Ocean. *Deep-Sea Res II* 48:3913–3941
- Owrid G, et al (2000) Spatial variability of phytoplankton, nutrients and new production estimates in the waters around Svalbard. *Polar Res* 19:155–171
- Rönner U, Sörensson F, Holm-Hansen O (1983) Nitrogen assimilation by phytoplankton in the Scotia Sea. *Polar Biol* 2:137–147
- Sañudo-Wilhelmy SA, Olsen KA, Scelfo JM, Foster TD, Flegal AR (2002) Trace metal distributions off the Antarctic Peninsula in the Weddell Sea. *Mar Chem* 77:157–170
- Siegel V (1988) Concept of seasonal variation of Krill (*Euphausia superba*) distribution and abundance west of the Antarctic Peninsula. In: Sahrhage D (ed) *Antarctic Ocean and resources variability*. Springer, Berlin Heidelberg New York, pp 219–230
- Sievers HA, Nowlin WD (1988) Upper Ocean characteristics in Drake Passage and adjoining areas of the Southern Ocean, 39°W–95°W. In: Sahrhage D (ed) *Antarctic Ocean and resources variability*. Springer, Berlin Heidelberg New York, pp 57–80
- Silva SN, Helbling EW, Villafañe V, Amos AF, Holm-Hansen O (1995) Variability in nutrient concentrations around Elephant Island, Antarctica, during 1991–1993. *Polar Res* 14:69–82
- Stein M (1988) Variation of geostrophic circulation off the Antarctic Peninsula and in the Southwest Scotia Sea, 1975–1985. In: Sahrhage D (ed) *Antarctic Ocean and resources variability*. Springer, Berlin Heidelberg New York, pp 81–91
- Sverdrup HU (1953) On conditions for the vernal blooming of phytoplankton. *J Cons Int Explor Mer* 18:287–295
- Veldkamp H (1976) Continuous culture in microbial physiology and ecology. Meadowland, Durham
- Westerlund S, Öhman P (1991) Iron in the water column of the Weddell Sea. *Mar Chem* 35:199–217
- Yamaguchi Y, Shibata Y (1982) Standing stock and distribution of phytoplankton chlorophyll in the Southern Ocean south of Australia. *Trans Tokyo Univ Fish* 5:111–128
- Zhou M, Niiler PP, Hu J-H (2002) Surface currents in the Bransfield and Gerlache Straits, Antarctica. *Deep-Sea Res I* 49:267–280